ICSV14
Cairns • Australia
9-12 July, 2007

14th International Congress on Sound & Vibration

EIGENVALUE VARIATION OF FUEL ROD EXPOSED TO UNIFORM AXIAL FLOW

Nam-Gyu Park[1], Joon-Kyu Park[1], Jung-Min Suh[1], Kyu-Tae Kim[1]

[1]R&D Center, Nuclear Fuel Technology Office, Korea Nuclear Fuel Co., LTD.
493, Deokjin-dong, Yuseong-gu, Daejeon, Korea
nkpark@knfc.co.kr

Abstract

Flow-induced vibration usually causes fretting wear in fuel rods during reactor operation, thus a prior knowledge on dynamics of fuel rod exposed to the flow condition should be provided. This work shows that dynamic characteristics of fuel rod depend on axial flow velocity. Assuming small lateral displacement, the effects of uniform axial flow are investigated. The results also show that axial flow generally reduces fuel rod stiffness and raises its damping in the normal condition. Solving generalized eigenvalue equation of the fuel rod system, the critical axial velocities at which the motion becomes unstable were found. Based on the simulation results, on the other hand, it turns out that the coolant flow in nuclear reactors rarely affect to the stability of nuclear fuel rod even in the severe condition.

1. INTRODUCTION

Fuel rods contain fissionable uranium pellets and are major components in a nuclear fuel assembly. A nuclear fuel assembly must support and locate the fuel rods such that adequate spacing is maintained for nuclear and hydraulic considerations. Generally, for PWR (Pressurized Water Reactor), the fuel assembly consists of hundreds of slender fuel rods that contain uranium pellets, spacer grids, and nozzles that accommodate reactor internals. Nuclear fission generates heat, and coolant flow should be provided to transfer the heat. Coolant flow, therefore, is indispensable for nuclear power generation, but it causes flow-induced vibration in fuel rods.

Flow-induced vibration is one of important design factors in nuclear fuel assembly design. Excessive vibration has fuel rods damaged, the topic has been a matter of interest during several decades. General solution of fuel rod flow-induced vibration cannot be found, since the coolant flow is not only turbulence but also a function of high pressure and temperature. It is usual that fuel rod behaviour can be estimated with empirical data or probabilistic methodology [1]. Analyzing flexible beam motion submerged in flow, Paidoussis [2~4] had accomplished remarkable results in the field of flow-induced vibration. Especially he calculated critical flow velocity which turns a beam with simple boundary condition to unstable. Based on the Paidoussious works, Chen and Wambsganss [5] studied the beam supported by torsion springs at the ends. Assuming the axial flow as potential flow, Chen [6] also computed added mass as a function of the distance from neighbouring rods, and vibration behaviour was discussed.

This work, assuming uniform axial flow, identifies some complex eigenvalues of fuel rod and studied critical flow velocity where the unstable motion begins. Unlike the previous works which concerned only on the beams with simple boundary conditions, the fuel rod with discretely spaced supports will be dealt.

2. CONFIGURATION OF A FUEL ROD

Figure 1 shows a schematic of fuel assembly and it consists of hundreds of fuel rods containing pellets. Fuel rods are supported by several spacer grids shown in Figure 2. At each cell in the spacer gird, a fuel rod is not allowed to move freely in the lateral and axial directions. Actually, every cell provides friction and geometric restriction with spring elements depicted in Figure 3. They elastically support the fuel rod at the beginning of power generation cycle. As cycle goes, they lose elasticity due to the relaxation mainly caused by neutron irradiation.

Fuel rod section properties are not uniform, since a fuel rod is composed of solid upper and lower plugs, a tube with uranium pellets, and a coil spring which is needed to restrict axial movement of the pellets. Fuel rod dimension is dependent on reactor configuration, but, the length is about 4 m and the diameter is around 10 mm for PWR. It is zirconium alloy that most fuel assembly components are made of, since fewer neutrons can be absorbed in zirconium.

Figure 4 shows a simplified fuel rod supported with discretely spaced grid supports, and it is exposed to uniform axial flow. In this work, only one lateral direction is considered. That is, it is assumed that the lateral motion is not interact with another lateral motion that is perpendicular to the page. Actually the two lateral motions are associated with friction forces, but the friction is ignored in this work.

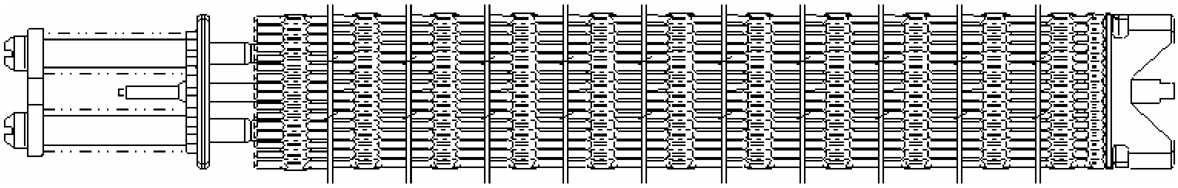

Figure 1. A fuel assembly with several spacer grids

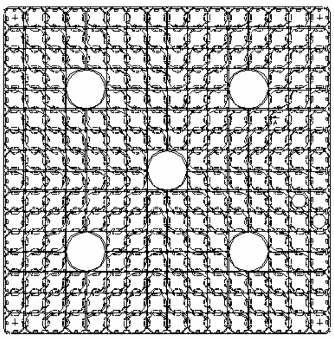

Figure 2. Plane view of spacer grid

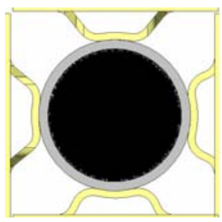

Figure 3. Cross section of cell in a typical grid structure; solid dark circle is the cross section of uranium pellet.

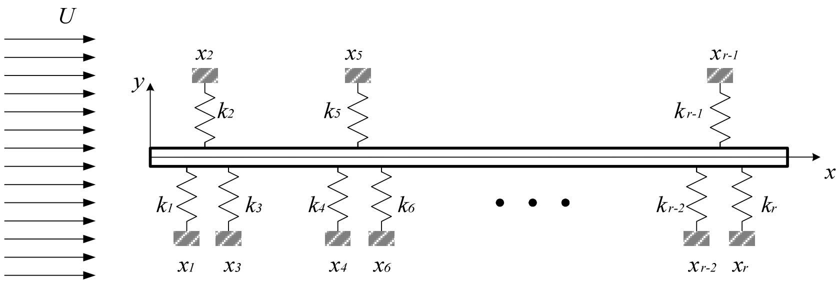

Figure 4. A simplified fuel rod model

3. DYNAMICS OF FUEL ROD IN AXIAL FLOW

Paidoussious [2] suggested a dynamic equation of flexible beam assuming small lateral beam displacement and uniform axial flow. Since the fuel rod, in the work, is supported by discretely spaced grids, spring elements are added to simulate the elastic supports shown in Figure 4. Equilibrium equation considering differential element in Figure 5 can be expressed as following.

$$\frac{\partial Q}{\partial x} - F_n - \sum_{i=1}^{r} k_i v \delta(x - x_i) - m_f \frac{D^2 v}{Dt^2} - m_r \frac{\partial^2 v}{\partial t^2} = 0 \tag{1}$$

Where Q is shear force, m_f and m_r is added flow mass per unit length and fuel rod mass per unit length, respectively. F_n means vertical component of fluid drag force, and it can be written [2] as

$$F_n = \frac{1}{2}\rho_f D U^2 c_f \frac{1}{U}\left(\frac{\partial v}{\partial t} + U\frac{\partial v}{\partial x}\right) \tag{2}$$

, where ρ_f, D, c_f , and U means fluid density, rod diameter, drag coefficient, and flow velocity respectively. The third term in Eq.(1) comes from discrete spring supports, and k_i is spring constant at the location x_i. $\delta(x- x_i)$ can be defined as Eq.(3).

$$\delta(x - x_i) = \begin{cases} 1, & if \;\; x = x_i \in \{x_1 \;\; x_2 \cdots x_r\} \\ 0, & otherwise \end{cases} \tag{3}$$

Considering axial flow only, material derivative of the fluid comes to

$$\frac{Dv}{Dt} = \frac{\partial v}{\partial t} + U\frac{\partial v}{\partial x} \tag{4}$$

Combining Eq.(1) ~ Eq.(4), and noting that the shear force is related to the third order differentiation of displacement leads to the dynamic equation of fuel rod in axial flow.

$$\frac{\partial^2}{\partial x^2}\left(E(x)I(x)\frac{\partial^2 v}{\partial x^2}\right) + \sum_{i=1}^{r} k_i v\delta(x - x_i) + m_f U^2\frac{\partial^2 v}{\partial x^2} + \alpha m_f U^2\frac{\partial v}{\partial x} + 2m_f U\frac{\partial^2 v}{\partial t\partial x} + \alpha m_f U\frac{\partial v}{\partial t} + (m_f + m_r)\frac{\partial^2 v}{\partial t^2} = 0 \tag{5}$$

Where α is $2c_f/\pi D$. Axial drag force could be developed in the fast moving flow, but it is ignored in this work. Especially, it is analytically and experimentally proved that pipe which conveys fluid does not carry axial drag force [7]. The third term in Eq.(5) can be seen at the beam equation when axial force is imposed at each end. The coefficient of the third term in Eq.(5), fluid flux, is equivalent to compressive force, and actually its dimension is that of force. We, thus, conjecture that natural frequencies will be decreased as flow velocity goes up. The fifth term in Eq.(5) is Coriolis force which damps out the motion, and it is caused by interaction between axially moving flow and rotating beam [7].

The boundary condition in the model depicted in Figure 4 is clearly free-free condition, but two different cases can be there when axial force is activated at both ends. The first candidate for boundary condition, illustrated in Figure 6(a), is that the flux is always perpendicular to the cross section at each end, thus no moment and shear force should be developed. The second shown in Figure 6(b) is that fluid flux is always constant in the magnitude and direction irrelevant to the end motion. The boundary condition for the latter, can be written

$$\frac{\partial}{\partial x}\left(E(x)I(x)\frac{\partial^2 v}{\partial x^2}\right)+m_f U^2\frac{\partial v}{\partial x}=0 \qquad (6)$$

It is notified that horizontal component of flux at the end is needed to define horizontal equation of motion.

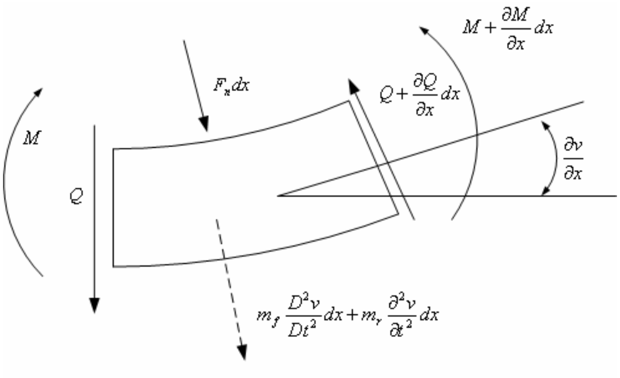

Figure 5. Free body diagram of a differential beam

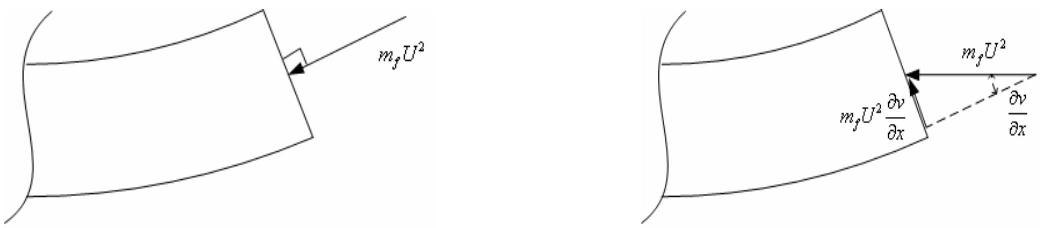

(a) applied force is always normal to the end sect ion

(b) applied force is always constant in direction and magnitude

Figure 6. Expected boundary conditions

4. FORMULATION OF EIGENVALUE EQUATION

It is difficult to solve Eq.(5) analytically. Thus, a discretized model should be introduced to compute the eigenvalues approximately. Multiplying a weighting function smooth enough to differentiate second times to both sides of Eq.(5), and subsequent integration results to the following variational equation.

$$\int_0^L E(x)I(x)\frac{\partial^2 w}{\partial x^2}\frac{\partial^2 v}{\partial x^2}dx+\int_0^L w\sum_{i=1}^r k_i v\delta(x-x_i)dx+m_f U^2\int_0^L w\frac{\partial^2 v}{\partial x^2}dx+\alpha m_f U^2\int_0^L w\frac{\partial v}{\partial x}dx+2m_f U\int_0^L w\frac{\partial^2 v}{\partial t\partial x}dx+$$
$$\alpha m_f U\int_0^L w\frac{\partial v}{\partial t}dx+\int_0^L w(m_f+m_r)\frac{\partial^2 v}{\partial t^2}dx=\left[\frac{\partial w}{\partial x}\left(E(x)I(x)\frac{\partial^2 v}{\partial x^2}\right)\right]_0^L-\left[w\left(\frac{\partial}{\partial x}E(x)I(x)\frac{\partial^2 v}{\partial x^2}\right)\right]_0^L \tag{7}$$

Where the terms in the right hand side of Eq.(7) prescribe free-free boundary condition. Another integration of the third term in Eq.(7) allows a symmetric matrix when finite element model is used, and arranging the equation results in Eq.(8).

$$\int_0^L E(x)I(x)\frac{\partial^2 w}{\partial x^2}\frac{\partial^2 v}{\partial x^2}dx+\int_0^L w\sum_{i=1}^r k_i v\delta(x-x_i)dx-m_f U^2\int_0^L \frac{\partial w}{\partial x}\frac{\partial v}{\partial x}dx+\alpha m_f U^2\int_0^L w\frac{\partial v}{\partial x}dx+$$
$$2m_f U\int_0^L w\frac{\partial^2 v}{\partial t\partial x}dx+\alpha m_f U\int_0^L w\frac{\partial v}{\partial t}dx+\int_0^L w(m_f+m_r)\frac{\partial^2 v}{\partial t^2}dx=\left[\frac{\partial w}{\partial x}\left(E(x)I(x)\frac{\partial^2 v}{\partial x^2}\right)\right]_0^L- \tag{8}$$
$$\left[w\left(\frac{\partial}{\partial x}E(x)I(x)\frac{\partial^2 v}{\partial x^2}\right)+wm_f U^2\frac{\partial v}{\partial x}\right]_0^L$$

The last term in the right hand side of Eq.(8) is equal to Eq.(6). And we see that vertical component of the fluid flux is imposed at the ends, and the boundary conditions at the ends are

$$E(x)I(x)\frac{\partial^2 v}{\partial x^2}=0 \tag{9}$$

$$\frac{\partial}{\partial x}\left(E(x)I(x)\frac{\partial^2 v}{\partial x^2}\right)+m_f U^2\frac{\partial v}{\partial x}=0 \tag{10}$$

Finally, finite element formulation with cubic polynomials is

$$([K]+[K]_1-[K]_2+[K]_3)\{d\}+([C]_1+[C]_2)\{\dot{d}\}+[M]\{\ddot{d}\}=\{0\} \tag{11}$$

, where each term is sequentially correspondent to every term in Eq.(8). It is noted that additional stiffness and damping matrices are appeared in Eq.(11), and it is resulted from axial flow. Laplace transform of Eq.(11), assuming 0 displacement and velocity as initial conditions, leads to

$$(s^2[M]+s[C]_T+[K]_T)\{Y\}=\{0\} \tag{12}$$

, where $[C]_T$ and $[K]_T$ means total damping and stiffness, respectively, and Y means Laplace transformation of displacement d. Rewriting Eq.(12) comes to

$$\left(\begin{bmatrix}[\mathrm{O}] & [K]_T\\ -[M] & [\mathrm{O}]\end{bmatrix}+s\begin{bmatrix}[M] & [C]_T\\ [\mathrm{O}] & [M]\end{bmatrix}\right)\begin{Bmatrix}s\{Y\}\\ \{Y\}\end{Bmatrix}=\{0\} \tag{13}$$

, where $[\mathrm{O}]$ is a matrix composed of all zero elements. Identifying the solution of the determinant equation of Eq.(13) gives eigenvalues, and their modes also can be found.

5. NUMERICAL SIMULATIONS AND DISCUSSION

5.1 Case 1 : absence of fluid damping and drag force

Damping and drag force were ignored to evaluate a few extreme cases. Material properties including density are defined based on reactor operating temperature, 300 °C . It has been investigated that neutron irradiation had material relaxed. Thus, not only the spring stiffness is decreased but also gap develops between the fuel rod and the springs in a cell. Actually the irradiation makes the system nonlinear, but nonlinearity is out of focus in the work. Instead, simulation for some severe case should be performed. That is, 0 spring stiffness condition will be examined.

When all spring supports work well, which corresponds to the beginning of power cycle, eigenvalues are computed with varying flow speed from 0. Figure 7 shows variation of the first eigenvalue, λ, where abscissa means real part of the eigenvalue and ordinate is imaginary part of it. Increasing flow velocity reduces the system stiffness, and we see that the eigenvalue moves to the origin along the ordinate as flow velocity increases. It is interesting to note that the eigenvalue exists on real axis when the flow is above a critical velocity. It is understood that excessive flow velocity induces negative stiffness and the motion will be unstable.

Table 1 shows critical velocities at which the unstable motion could occur. The first case is that every support works well, which was described as above. The second and the last cases are that every grid except top and bottom grids does not work. Actually the top and bottom grids are made of different material from that of mid grid to avoid irradiation induced relaxation. For the first case, the critical velocity is above 100 m/sec, but it is far away from operating condition and is not realistic. In real world, about 12 m/sec coolant flow is provided to a reactor. The flow passing through reactor lower internals lost its initial energy, and finally 6 m/sec coolant flow is supplied to fuel assemblies. It is, therefore, concluded that unstable rod motion is barely seen in real situation.

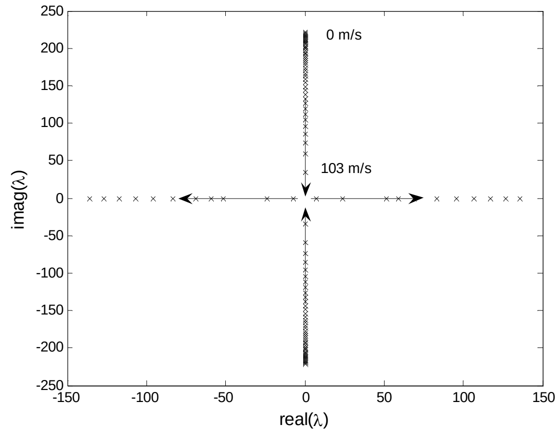

Fig.7 Variation of the first modal frequency(X) in a fully supported condition

Table 1 Critical velocity

Case description	Critical velocity (m/sec)
Fully supported	106.6
Top & Bottom grid supports only	18.2
Bottom grid support only	7.6

5.2 Case 2 : existence of fluid damping and drag force

To compute additional damping caused by flow, the severe case - bottom grid only works - was simulated. Structural damping was neglected and 0.2 of drag force coefficient was chosen. Table 2 lists the first five damping ratios and it can be seen that damping is raised as flow velocity become higher. Figure 8 shows variation of the first two eigenvalues. When flow velocity is 0, every real part is 0. For the second eigenvalue, we see that the real part of the eigenvalue is positive above 19.8 m/sec. Actually, passing through the velocity, the system turns to unstable, but the velocity level is three times higher than real situation.

Note that the first two eigenvalues are not continuous as delineated in Figure 8, that is the first and the second eigenvalues show jumps around 9~10 m/sec flow. The crossing modes can be observed at the flow velocity, and overlaying the two figures shows crossing modes clearly.

Table 2 Expected damping ratio with respect to axial flow velocity

U (m/sec)	ς_1	ς_2	ς_3	ς_4	ς_5
1.5	0.562	0.135	0.050	0.026	0.026
3.0	0.664	0.263	0.099	0.052	0.052
4.6	0.639	0.383	0.149	0.078	0.078
6.1	0.538	0.527	0.199	0.105	0.105
7.6	0.385	0.670	0.250	0.132	0.132

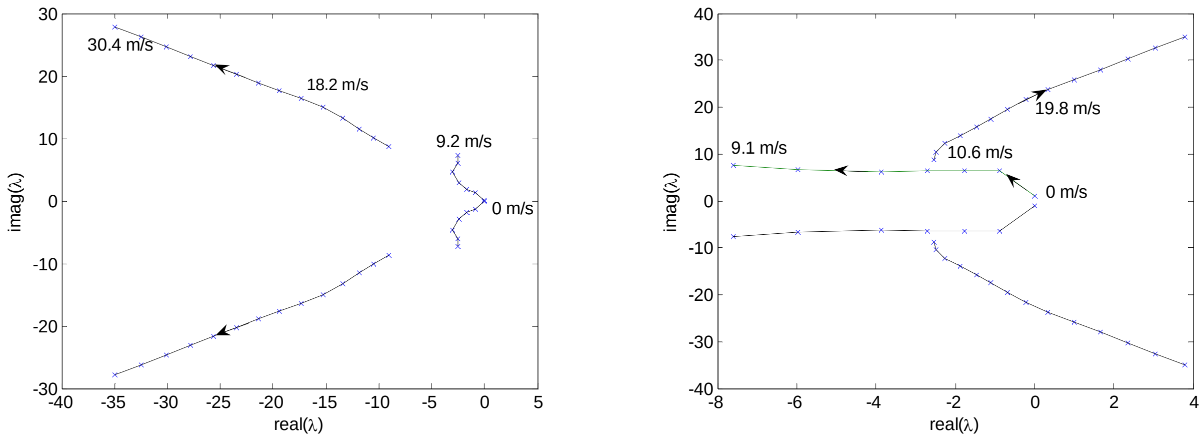

(a) first eigenvalue (b) second eigenvalue

Fig.8 Variation of eigenvalues

6. CONCLUSIONS

This work studied eigenvalue variation of fuel rod exposed to uniform axial flow. The fuel rod structure was simplified to a beam with discretely spaced elastic supports, and variational equation including boundary conditions was investigated.

According to the simulation results, it is concluded that dynamic properties of fuel rod are dependent on flow velocity. It is also discussed that the critical flow velocity which makes the fuel rod unstable is above the normal velocity. In addition, considering fluid damping, unstable motion is rarely expected.

It should be notified that the results in the study were based on some assumptions such as uniform axial flow. Realistic situations including fluid with air bubbles and cross flow should be the future work for more detailed analysis.

ACKNOWLEDGEMENT

This work was funded primarily by KOREA Ministry of Commerce, Industry and Energy (Project Number : R-2005-1-391), and we would like to express our gratitude to the governmental organization.

REFERENCES

[1] M. K. Au-Yang, *Flow-Induced Vibration of Power and Process Plant Components*, Professional Engineering Publishing, 2001.

[2] M. P. Paidoussis, "Dynamics of Flexible Slender Cylinders in Axial Flow; Part 1 Theory", *J. Fluid Mech.* **26**, 717-736 (1996).

[3] M. P. Paidoussis, "Dynamics of Flexible Slender Cylinders in Axial Flow; Part 2 Experiments", *J. Fluid Mech.* **26**, 737-752 (1996).

[4] M. P. Paidoussis, "An Experimental Study of Vibration of Flexible Cylinders Induced by Nominally Axial Flow", *Nuclear Science and Eng.* **35**, 127-138 (1969).

[5] S. S. Chen, M. W. Wambsganss, "Parallel Flow Induced Vibration of Fuel Rods", *Nuclear Eng. and Design* **18**, 253-278 (1972)

[6] S. S. Chen, "Vibration of Nuclear Fuel Bundles", *Nuclear Eng. and Design* **35**, 399-422 (1975).

[7] M. P. Paidoussis, Fluid-Structure Interactions ; Slender structures and Axial Flow Volume 1, *Academic press*, 1988.